The PERC+ cell: More output power for less aluminium paste

Thorsten Dullweber, **Christopher Kranz**, **Robby Peibst**, **Ulrike Baumann** & **Helge Hannebauer**, Institute for Solar Energy Research Hamelin (ISFH), Emmerthal, & **Alexander Fülle**, **Stefan Steckemetz**, **Torsten Weber**, **Martin Kutzer**, **Matthias Müller**, **Gerd Fischer**, **Phedon Palinginis** & **Holger Neuhaus**, SolarWorld Innovations GmbH, Freiberg, Germany

ABSTRACT

Passivated emitter and rear cell (PERC) technology has been forecast to become mainstream in the next few years, gaining around a 30% market share. This paper presents a novel PERC solar cell design in which a screen-printed rear aluminium (Al) finger grid is used instead of the conventional full-area Al rear layer, while implementing the same PERC manufacturing sequence. This novel cell concept, called 'PERC+', offers several advantages over PERC. In particular, the Al paste consumption for PERC+ cells is drastically reduced to 0.15g per wafer, as opposed to 1.6g per wafer for conventional PERC cells. The aluminium back-surface fields (Al-BSFs) created by the Al fingers are 2µm deeper, which increases the open-circuit voltage by 3mV. Moreover, the five-busbar Al finger grid enables the use of PERC+ cells in bifacial applications, offering front-side efficiencies of up to 21.2% and rear-side efficiencies of up to 16.6%, measured with a black chuck, and a corresponding bifaciality of up to 78%. When a reflective brass chuck is used for measurement, PERC+ cells demonstrate efficiencies of up to 21.5%, compared with 21.1% for conventional PERC cells. The PERC+ efficiency is higher, since the deeper aluminium back-surface field (Al-BSF) increases the open-circuit voltage and also because the reflective brass chuck increases the internal rear reflectance, leading to higher short-circuit currents. PERC+ cells are therefore expected to be an attractive candidate for both bifacial glass–glass modules and monofacial modules with a white backsheet. While ISFH developed the aforementioned PERC+, SolarWorld independently pioneered a very similar bifacial PERC+ cell process that has been successfully transferred to mass production. Novel glass–glass bifacial PERC+ modules based on a very simple, lean and cost-effective bifacial cell process were launched at Intersolar 2015. These new bifacial PERC+ modules have demonstrated an increase in annual energy yield between 5 and 25% in simulations, which has also been confirmed by the first outdoor measurements.

Introduction

Passivated emitter and rear cells (PERCs) are currently being introduced into mass production by several leading solar cell manufacturers, such as SolarWorld, Hanwha Q-Cells, Trina Solar and others [1–5]. In May 2015 SolarWorld demonstrated a record efficiency of 21.67% with an industrial p-type Cz-Si five-busbar PERC solar cell, an achievement that was externally certified by Fraunhofer-ISE CalLab in Germany. The latest photovoltaic technology roadmap ITRPV forecasts a market share for PERC solar cells of 35% by 2019 [6]. These industrial PERC cells use p-type wafers and a full-area screen-printed aluminium (Al) rear layer, which only locally contacts the silicon wafer in areas where the rear passivation has been removed by laser contact opening (LCO). Furthermore, the lab-type PERC cell of Blakers et al. in 1989 [7] employed a full-area evaporated Al rear contact. Full-area aluminium layers, however, consume a large amount of Al paste of around 1.0 to 1.5g per wafer; they also prevent any transmission of sunlight from the rear side into the silicon wafer, and hence any bifacial applications of these industrial PERC cells are ruled out.

> "ITRPV predicts a market share for bifacial solar cell technologies of 15% by 2019."

Bifacial solar cell concepts, on the other hand, are increasingly drawing a lot of interest for use in various applications, particularly in PV power plants, where the electricity produced can be increased by up to 20% using bifacial instead of monofacial solar cells [8,9]. Accordingly, the photovoltaic technology roadmap ITRPV predicts a market share for bifacial solar cell technologies of 15% by 2019 [6].

At the moment, industrial bifacial solar cell concepts mainly use n-type wafers, such as passivated emitter and rear totally diffused (PERT) solar cells [10–13] or heterojunction solar cells [14,15]. One of the challenges of these two cell concepts is that they typically involve screen-printed silver (Ag) finger grids on both sides of the wafer, and hence the consumption of a large amount of expensive Ag paste. Moreover, n-PERT cells entail single-sided boron and phosphorus doping, which requires additional or alternative process steps compared with p-type PERC cell processing.

Bifacial silicon solar cell concepts using p-type wafers and a screen-printed Al rear finger grid have also been under investigation. In 2001 ISFH introduced a bifacial p-type solar cell in which the rear Al grid fires through the SiN_x rear passivation layer without using any LCO or rear-side boron doping [16]; ECN further developed this approach, offering the so-called 'p-PASHA' cell concept [17,18]. The published efficiencies, however, are very similar to those obtained with full-area Al-BSF cells, but are significantly lower than those of typical industrial PERC cells.

Recently, the company RCT Solutions reported a bifacial PERCT cell concept using p-type multicrystalline wafers, LCO and a screen-printed Al finger grid, resulting in front-side efficiencies of up to 18.6% [19,20]. However, this entailed an additional BBr_3 diffusion for the PERCT rear-side doping [19,20], which may increase the number of process steps compared with conventional monofacial PERC cell processing.

This paper presents high-efficiency bifacial PERC solar cells fabricated at ISFH SolarTeC using a typical

industrial PERC process flow (e.g. with AlO_x/SiN_y rear passivation and LCO, but without rear boron doping), involving the application of a screen-printed Al finger grid on the rear side instead of a full-area Al layer. In the past, the low conductivity of screen-printed Al has been a concern for Al finger grid designs. However, with modern Al pastes, and in particular the use of a greater number of busbars (such as five-busbar H-pattern designs [21,22]), the Al conductivity is no longer a major limitation, as will be explored in this paper.

In the work reported here, the impact of the Al finger grid on the Al paste consumption and on the Al–Si contact formation was investigated. The front- and rear-side efficiencies of the resulting bifacial PERC solar cells were measured, and the implications of a white backsheet for its use in conventional monofacial modules were studied. This novel PERC cell design with screen-printed rear Al grid has been named 'PERC+', where the '+' indicates the inherent advantages reported in this paper of the Al finger grid compared with a full-area Al rear metallization. In parallel to the aforementioned R&D activities at ISFH, SolarWorld independently pioneered the bifacial PERC+ cell process, with feasibility studies starting in 2014. This paper reports on the successful transfer to mass production of PERC+ cells at SolarWorld as well as on the novel glass–glass bifacial modules incorporating these cells. The added value to the PV industry of bifacial modules based on a very simple, lean and cost-effective bifacial cell process is discussed.

PERC+ solar cell process at ISFH

Boron-doped, 2Ωcm, 156mm × 156mm, Czochralski-grown silicon wafers are used in the work reported in this paper. After cleaning, the rear side is coated with a protection layer, which acts as a barrier in the subsequent alkaline texturing and phosphorus diffusion, resulting in an emitter sheet resistance of 100Ω/sq. The rear protection layer and the phosphorus glass are removed by wet chemistry. An AlO_x/SiN_y stack is deposited as the rear surface passivation. The thickness of the SiN_y capping layer is set to 80nm to obtain low reflection of the rear side of the bifacial PERC+ cells; the monofacial reference PERC cells with full-area Al layer receive a 200nm-thick SiN_y capping layer. The front side is passivated with plasma-enhanced chemical vapour deposition (PECVD) SiN_x. Line-shaped LCOs are formed on the PERC+ rear side, with a pitch p exceeding that of the monofacial PERC cells by a factor of 1.5; the larger LCO pitch of PERC+ cells is intended to reduce the rear metal coverage, thereby reducing the shadowing loss when the rear side receives illumination.

The Ag front grid is printed using a dual-print process similar to that described in Hannebauer et al. [21]: first the five busbars are screen-printed using a non-firing-through Ag paste, and then the Ag fingers are printed with a stencil using a firing-through Ag paste. For the Al screen print, a commercially available Al paste is used. The monofacial reference PERC cells are full-area screen printed, whereas the bifacial PERC+ cells use an Al finger grid screen design with a five-busbar H pattern. The aluminium screen has a finger opening width of 100µm and a pitch identical to the LCO pitch. The Al finger opening width is significantly wider than the LCO widths; hence, the Al–Si rear contact width and the Al grid line width can be optimized individually by the LCO and Al screen parameters. In the case of PERC+ cells, the Al fingers are printed in alignment with the LCOs.

As shown in Table 1, the monofacial PERC cells (group 1) consume 1.6g of Al paste per wafer, measured directly after printing, while the Al paste consumption of the bifacial PERC+ cells (group 2) is dramatically reduced to 0.15g per wafer, because of the finger grid design. The front and rear contacts are fired in a conventional belt furnace, during which the Al paste locally alloys with the silicon wafer in areas where the rear passivation has been removed by laser ablation.

> "Al paste consumption of the bifacial PERC+ cells is dramatically reduced to 0.15g per wafer, because of the finger grid design."

Schematic drawings of the resulting bifacial PERC+ and monofacial PERC solar cells are presented in Fig. 1; photographs of the front and rear surface of the PERC and PERC+ solar cells are shown in Fig. 2. Table 1 summarizes the various PERC and PERC+ process parameters.

Aluminium finger grid properties

The Al finger geometries of the PERC+ solar cells are analysed using a light microscope and an optical profilometer after firing. The Al finger height is similar to that of the full-area Al layer. The final Al finger widths are much wider than the 100µm screen-opening width, since the Al paste is not optimized for high aspect ratio prints. The Al finger width corresponds to an area fraction of 12.6% of the Al fingers on the PERC+ cell. If the area fraction of the five aluminium busbars of 1.6% is taken into account, the total metallization area fraction of the Al finger grid works out at 14.2%.

The wafer bow of four PERC and five PERC+ solar cells is measured as the maximum value of the distance of the solar cell to a flat surface. The bifacial PERC+ cells are almost perfectly flat, with a wafer bow of only 0.2±0.1mm, whereas the monofacial PERC cells exhibit a wafer bow of 2.5±0.5mm. This is to be expected, since the bifacial PERC+ cells are fairly symmetric, with both wafer surfaces being coated with dielectric layers and metal grid lines, thus reducing the mechanical stress within the wafers compared with PERC cells with a full-area Al layer.

In order to assess the impact of the Al grid design on the series resistance of the PERC solar cells, the grid line resistance of the Al fingers

Group	Solar cell type	Rear SiN thickness [nm]	LCO pitch [a.u.]	Al finger width [µm]	Al area fraction [%]	Al paste consumption [g]
1	PERC	200	p	N/A	100	1.6
2	PERC+	80	1.5 p	100	14.2	0.15

Table 1. PERC and PERC+ process parameters. Although the principal process flows for the two types of cell are identical, several process parameters were adjusted for the PERC+ cell in order to optimize the bifaciality. (The Al finger width refers to the Al screen-opening width, and the Al area fraction includes the fingers and busbars.)

is determined by four-point probe measurements on final PERC+ solar cells and on test wafers with and without LCOs below the Al fingers. When the finger length and the average cross-sectional area of the Al fingers as measured with an optical profilometer are taken into account, the calculation of the specific resistivity of the Al fingers works out to be 20±5μΩcm. Interestingly, very similar values are obtained with and without LCOs beneath the Al fingers, indicating that the Al–Si eutectic layer below the Al fingers provides only a minor contribution to the lateral conductivity. The series resistance contribution of the Al finger grid, calculated on the basis of the layout and the specific resistivity, is 0.1Ωcm^2; this represents a relative increase of 20% compared with the total series resistance of 0.55Ωcm^2 of the monofacial reference PERC cells. The relatively small resistance contribution of the Al finger grid, despite the rather high specific resistivity, is a consequence of the five-busbar grid design, which reduces the grid line resistance because of the reduced finger length compared with conventional three-busbar designs [22].

Another interesting aspect is the impact of the Al finger grid on the Al–Si contact formation and, in particular, on the depth of the Al-BSF. Fig. 3 shows two typical scanning electron microscope (SEM) images of the resulting local aluminium contacts for the monofacial reference PERC cell as well as for the bifacial PERC+ cell: the depth of the Al-BSF of the monofacial reference PERC cell (Fig. 3(a)) is 3.5±1.5μm (taken as the average value of eight measured local Al contacts), whereas the bifacial PERC+ cell (Fig. 3(b)) exhibits Al-BSF depths of 5.5±1.5μm [23]. The increased Al-BSF depth in the case of the bifacial PERC+ cell is due to the Al finger layout. During furnace firing, silicon from the wafer diffuses through the laser contact opening into the Al paste layer [24]. During the cool-down phase, the liquid silicon in the aluminium layer epitaxially regrows at the silicon wafer surface, incorporating Al up to the solid-solubility limit, thereby forming the Al-BSF.

In the full-area Al layer, the area of high silicon content is 520μm wide, as can be observed in the darker busbar area on the light microscope image in Fig. 4. The wide Si out-diffusion leads to low silicon concentrations in the aluminium layer, and hence to shallow Al-BSF depths. This effect has been quantitatively described in Müller et al. [25] and Lauermann et al. [26]. In contrast, in the case of the PERC+ cells, the Al finger confines the silicon diffusion to the Al finger width, as illustrated in Fig. 4, leading to higher silicon concentrations in the Al finger, and hence deeper Al-BSFs. Additionally, for the PERC+ cells the depth of the Al–Si eutectic layer is found to be shallower than for the PERC cells, as seen in Fig. 3; moreover, the number of voids in the local Al contacts is significantly reduced for the PERC+ cells compared with the PERC cells. It is very likely that both effects are a consequence of the confinement of the silicon diffusion of the Al grid, since the higher Si content in the Al grid reduces the chemical potential gradient that drives the Si diffusion from the silicon wafer to the Al finger. The reduced number of voids contributes to the deeper Al-BSF of the PERC+ cells, since quite often voids cause locally shallower Al-BSFs. The deeper Al-BSF lowers the contact recombination [27] and hence potentially enables higher open-circuit voltages to be obtained with PERC+ solar cells.

> "The deeper Al-BSF lowers the contact recombination and hence potentially enables higher open-circuit voltages to be obtained with PERC+ solar cells."

I–V parameters of bifacial PERC+ solar cells processed at ISFH

The current–voltage (*I–V*) parameters of the PERC and PERC+ cells under study are measured in-house at ISFH directly after processing, since previous results [28] have shown that PERC cell efficiencies measured directly after processing are comparable to the efficiencies measured after boron-oxygen deactivation (e.g. by thermal treatment). The monofacial PERC solar cells are measured using a reflective brass chuck, which electrically contacts the full rear surface of the solar cell. The *I–V* tester is calibrated using an ISE CalLab certified monofacial reference PERC solar cell.

The best monofacial PERC cell of group 1 in Table 1 achieves 21.1% efficiency η, as shown in Table 2; the average efficiency of all five corresponding PERC cells is 20.9%.

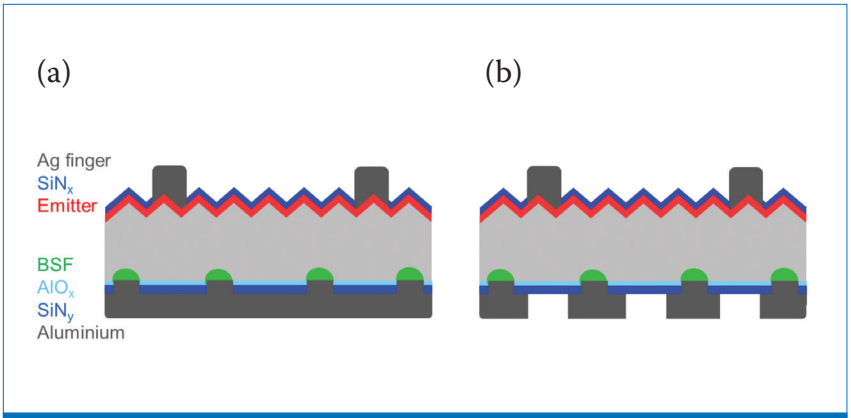

Figure 1. Cell schematics: (a) typical industrial monofacial PERC solar cell with full-area Al rear layer; (b) bifacial PERC+ solar cell with rear Al finger grid. (Diagrams are not to scale.)

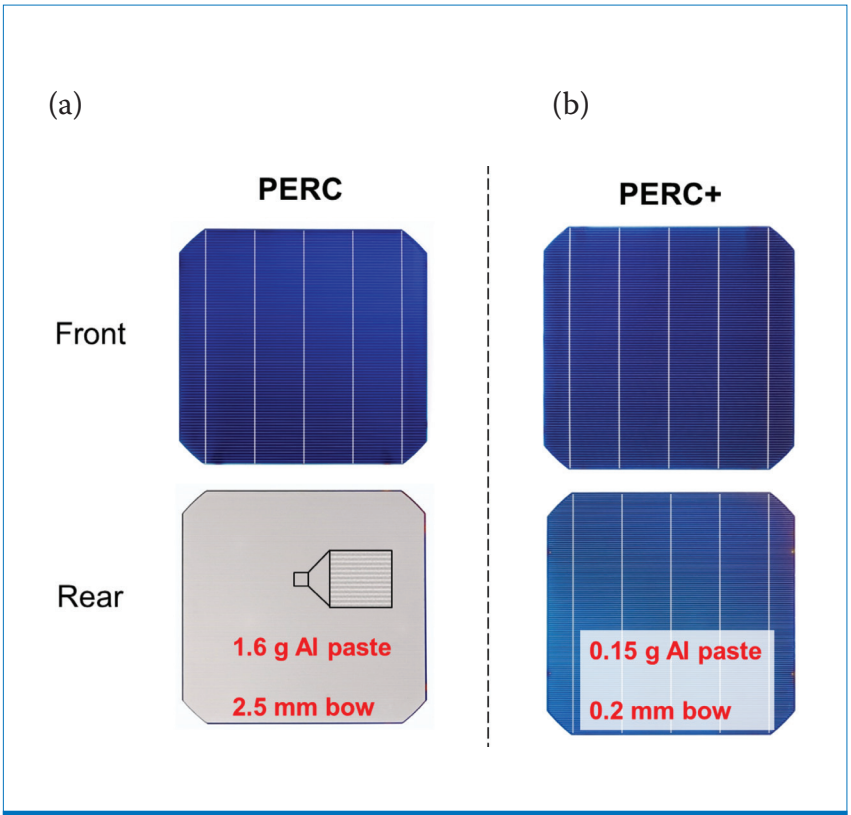

Figure 2. Photographs of the front and rear sides of (a) a typical industrial monofacial PERC solar cell with full-area Al rear layer, and (b) a bifacial PERC+ solar cell with rear Al finger grid. The Al finger grid design of the PERC+ cell enables bifaciality and drastically reduces the Al paste consumption from 1.6g to 0.15g per wafer; moreover, the PERC+ cells exhibit almost no wafer bow in contrast to conventional PERC cells.

The bifacial PERC+ cells are measured in-house at ISFH using the same *I–V* tester and the same calibration method as for the monofacial PERC cells. When the reflective brass chuck, which contacts the full-rear Al grid, is used, the best PERC+ cell demonstrates 21.5% efficiency, as shown in Table 2 [29]. The average efficiency of all seven corresponding PERC+ cells is 21.0%.

The short-circuit current density J_{sc} for the PERC+ cell is 40.1mA/cm^2, and hence slightly higher than the J_{sc} of 39.8mA/cm^2 for the PERC cell. The open-circuit voltage V_{oc} for the PERC+ cell is 666mV, and hence 6mV higher than the V_{oc} of 660mV for the monofacial PERC solar cell. The higher V_{oc} of the PERC+ cells is due partly to the deeper Al-BSF (as shown in Fig. 3) and partly to the larger LCO pitch of the PERC+ cells (see Table 1).

The PERC+ cells exhibit on average a 0.5% abs. lower *FF* and a 0.13Ωcm^2 higher series resistance R_s compared with the average values for the monofacial PERC cells when both are measured with the full-area contacting brass chuck. This difference in series resistance is due to the larger LCO pitch (see Table 1) of the PERC+ cells, which (according to the model of Saint-Cast [30]) increases the spreading resistance of the wafer bulk from 0.2Ωcm^2 for the PERC cells to 0.3Ωcm^2 for the PERC+ cells.

To assess the bifacial performance of the PERC+ cells, for example when installed in bifacial glass–glass modules, the PERC+ cells are measured using a black chuck, where the front and rear metal grids are contacted at only the five busbars, and not at the fingers. With front-side illumination (Ag metal grid), the PERC+ cell in Table 2 achieves an efficiency of 21.2%, which is 0.3% abs. lower than the corresponding *I–V* measurement with the brass chuck. The reasons for this are twofold: 1) the J_{sc} is 0.2mA/cm^2 lower when measured with a black chuck, since the reflected light of the brass chuck is absent; 2) the *FF* is on average 0.4% lower when measured with the black chuck, since now the resistance of the Al finger grid contributes to the total series resistance R_s. The average R_s value of all PERC+ cells when measured with the black chuck was found to be 0.77Ωcm^2, and hence 0.12Ωcm^2 higher than the measurement with the brass chuck. This measured value corresponds well to the calculated series resistance of the Al finger grid of 0.10Ωcm^2, as explained in the previous section.

When illuminated from the rear side (Al metal grid), the PERC+ cells exhibit

efficiencies of up to 16.6%, as shown in Table 2. The short-circuit current J_{sc} is only 31.3mA/cm^2, and hence 8.6mA/cm^2 lower than the measurement with front-side illumination; this is the main reason for the considerably lower rear-side efficiency. The V_{oc} values of the PERC+ cells when illuminated from the rear are 6mV lower than with front-side illumination, which is a result of the lower J_{sc}. The root cause of the slightly higher *FF* values with rear illumination is not yet understood. The front- and rear-side efficiencies of respectively 21.2% and 16.6% correspond to a bifaciality $B = \eta_{rear}/\eta_{front}$ = 78%. Other PERC+ cells of this batch demonstrated slightly higher bifacialities, of up to 80%

Quantum efficiency and reflectance of bifacial PERC+ solar cells

The internal quantum efficiency (IQE) and the reflectance of the monofacial PERC solar cell in Table 2 are measured using a brass chuck, whereas for the PERC+ cell in Table 2 a black chuck illuminated from the front side is used. As shown in Fig. 5, both the IQE (top curves) and the reflectance (bottom curves) of the PERC and PERC+ cells are very similar. However, at a wavelength of around 1,100nm, the PERC+ cell exhibits slightly higher IQE values than those for PERC cells, indicating reduced carrier recombination at the rear surface or rear Al contacts in the case of the PERC+ cells.

The reflectance of the PERC+ cell is then measured again by gluing a white backsheet foil onto the black measurement chuck. This measurement set-up is intended to assess the effective rear-side reflectance of the PERC+ cells when used in conventional modules with a white backsheet. As can be seen in Fig. 5, the reflectance increases from 0.44 to 0.51 at a wavelength of 1,200nm when measured with a white backsheet instead of the black chuck.

The values for the rear reflectance Rb, the Lambertian fraction Λ, and the effective rear-surface recombination velocity S_{rear} are extracted by means of analytical modelling [31]; these are summarized in Table 3.

The S_{rear} values for the PERC cells are around 100 cm/s; the PERC+ cells achieve S_{rear} values below 40cm/s, which is the resolution limit for this methodology, indicating that Al contact recombination is reduced because of the increased Al-BSF depth.

The Rb values of around 88% are

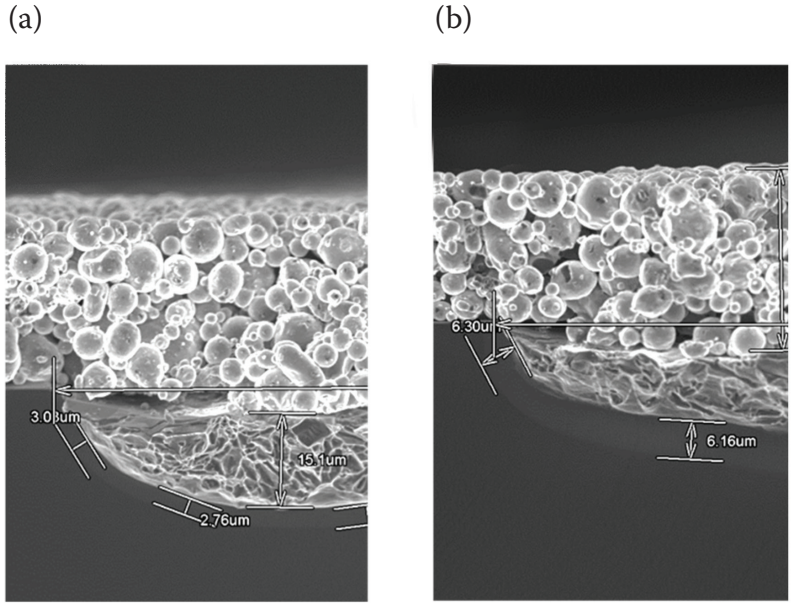

Figure 3. SEM images of the local aluminium contacts: (a) monofacial reference PERC cell; and (b) bifacial PERC+ cell. The deeper Al-BSF of the bifacial PERC+ cells is a result of confinement of the silicon diffusion to the Al finger width (as shown in Fig. 4).

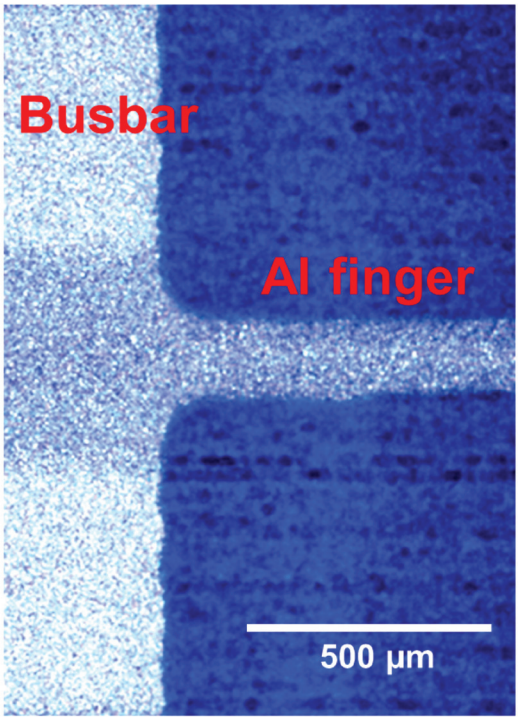

Figure 4. Light microscope image of the Al finger grid, displaying a part of the busbar on the left and one Al finger on the right. The darker area in the middle of the busbar shows the area of increased silicon content in the Al paste, caused by the Si diffusion from the wafer through the LCO into the Al paste during furnace firing. The width of the area with high Si content is in the range of 520µm and hence similar to that for PERC cells with full-area rear Al layer. In contrast, the Al finger confines the Si diffusion to the Al finger width, resulting in higher Si concentrations in the Al paste during furnace firing, and hence in deeper Al-BSFs (as seen in Fig. 3).

Group	Solar cell type	Al area fraction [%]	Side of illumination	Chuck type	η [%]	J_{sc} [mA/cm^2]	V_{oc} [mV]	FF [%]	R_s [Ωcm^2]
1	PERC	100	Front	Brass	21.1	39.8	660	80.5	0.53
2	PERC+	14.2	Front	Brass	21.5	40.1	666	79.7	0.55
2	PERC+	14.2	Front	Black	21.2	39.9	666	79.1	0.67
2	PERC+	14.2	Rear	Black	16.6	31.3	660	80.7	0.60

Table 2. Solar cell parameters measured at ISFH under AM1.5 standard test conditions of the best monofacial PERC cell of group 1 and of the best bifacial PERC+ cell of group 2 in Table 1. Both cells were measured using a brass chuck; additionally, the PERC+ cell was measured using a black chuck that was illuminated from either the front or the rear, in order to assess the bifaciality.

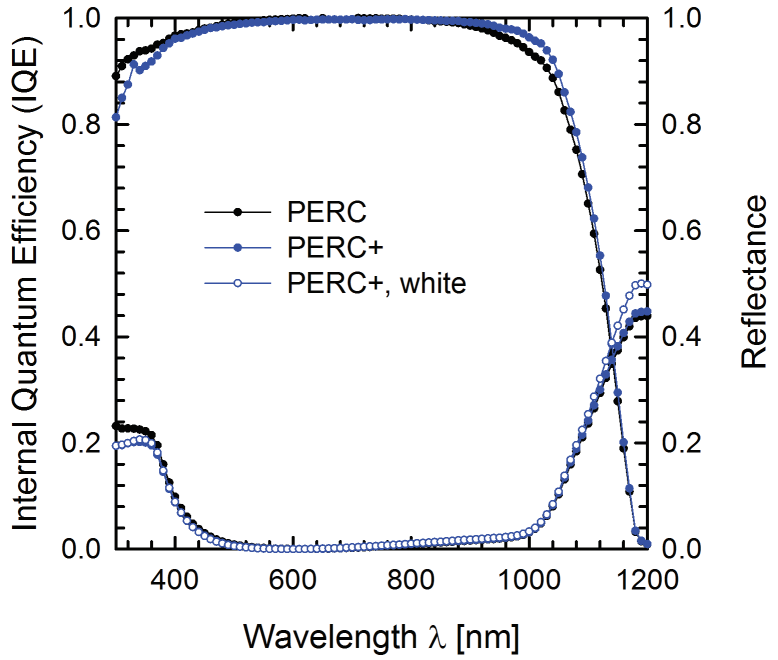

Figure 5. IQE (top curves) and reflectance (bottom curves) of the bifacial PERC+ cell and the monofacial PERC cell in Table 2, measured with front-side illumination (Ag grid). For both IQE and reflectance, the PERC cell was measured using a brass chuck, whereas the PERC+ cell was measured using a black chuck. Additionally, the reflectance of the PERC+ cell with a white backsheet glued on the chuck was measured, resulting in the highest reflectance in the long-wavelength regime.

very similar for both PERC+ cells (measured with a black chuck) and monofacial PERC cells. The Rb value increases to 90.4%, however, when the PERC+ cell is measured with the white chuck. The increase in Rb from 88.1% (black chuck) to 90.4% (white chuck) corresponds to an increase in J_{sc} of 0.17mA/cm^2, as calculated with the solar cell analysis software SCAN, which was developed in-house and uses the analytical model for the QE introduced in Brendel et al. [31]. This value is in good agreement with the measured increase in J_{sc} of 0.2mA/cm^2 when the I–V measurements of the PERC+ cell in Table 2 with a brass chuck and a black chuck are compared.

Pilot production of bifacial PERC+ cells at SolarWorld

As mentioned earlier, in parallel to the bifacial PERC+ development at ISFH, SolarWorld has been independently pursuing the bifacial PERC+ cell process, described in this section, with feasibility studies on their Solar Cell Pilot Line at SolarWorld Innovations having begun in 2014. The monofacial production baseline PERC solar cell process was modified to achieve suitable bifaciality of the resulting cells, without major modifications of the well-established production process. A transfer to mass production (announced at the end of 2014 [32]) has been successfully accomplished, and novel glass–glass bifacial modules based on this bifacial PERC+ cell variant were launched at Intersolar 2015 [33], introducing the added value to the PV industry of bifacial modules based on a very simple, lean and cost-effective bifacial cell process.

Starting with the monofacial production baseline PERC solar cell process, the following process steps have been modified: 1) the SiN capping layer of the rear passivation; 2) the ablation pattern of the contact openings; and 3) the Al grid. The bifacial PERC+ solar cell process was tested in a pilot production run, consisting of 100,000 bifacial cells with three busbars, on the PERC solar cell production line at SolarWorld. The average I–V parameters of the bifacial PERC+ solar cells are very similar to those of the monofacial PERC production baseline. The efficiency of the PERC+ solar cells is marginally lower (1.5% rel.) than that of the monofacial PERC cells; the reasons for this are mainly the increased series resistance of the Al grid compared with a full-area Al contact and the inferior passivation quality of the rear stack with a reduced thickness of the SiN capping layer. The bifaciality $B = \eta_{rear}/\eta_{front}$ of the PERC+ cells is in the range 63–65%. Process development is ongoing in order to increase front-side efficiencies and bifaciality. Transparent glass–glass modules were built from these bifacial PERC+ cells: Fig. 6 gives a visual impression of a module from the rear and front sides. Note that the module bifaciality is higher than the cell bifaciality because of light-trapping effects.

In order to analyse the consumer benefits of the bifacial PERC+ modules, simulations of the annual energy yield

Group	PERC type	Chuck type	R_b [%]	Λ [%]	S_{rear} [cm/s]
1	PERC	Brass	87.8	69.2	128
2	PERC+	Black	88.1	67.4	< 40
2	PERC+	White	90.4	67.8	–

Table 3. Rear reflectance R_b, Lambertian fraction Λ, and effective rear-surface recombination velocity S_{rear}, as extracted from the IQE and reflectance measurements of the PERC and PERC+ cells in Fig. 5. The PERC+ cell measured with a white backsheet yields the highest R_b value of 90.2%, demonstrating the benefit of the external rear reflector, as sketched in Fig. 8(b)).

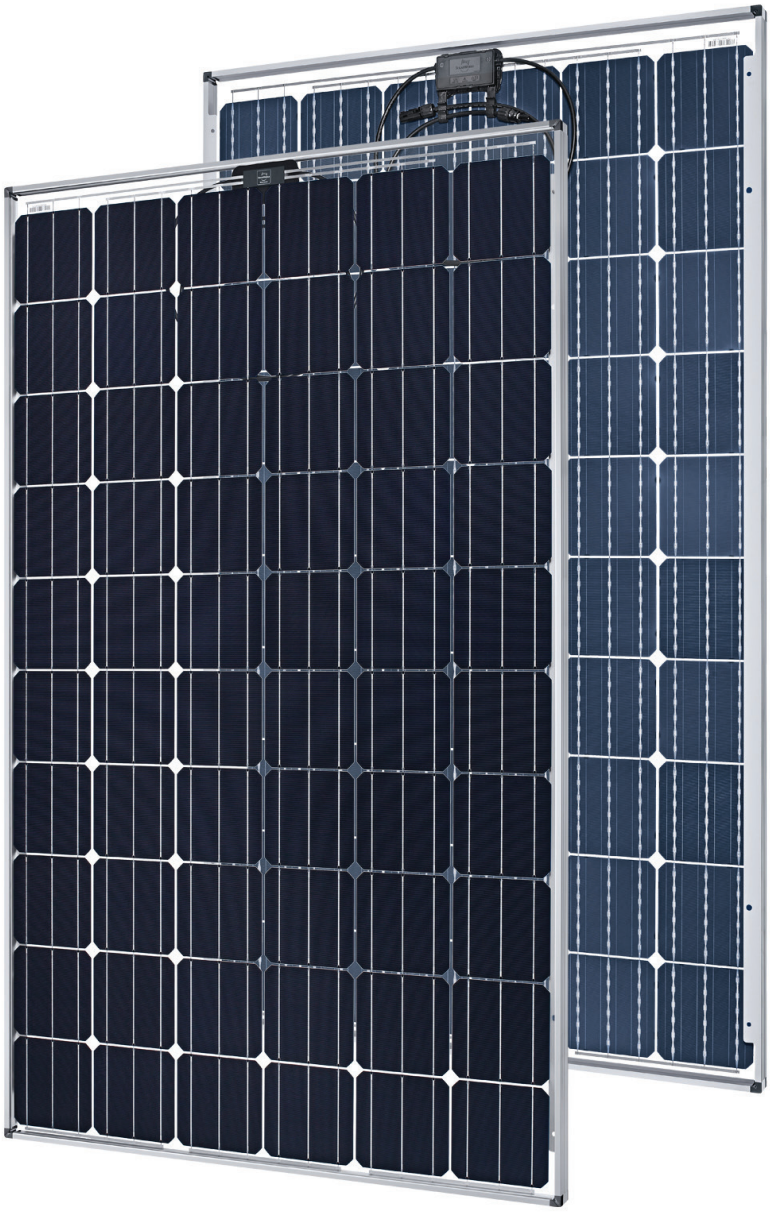

Figure 6. Rear and front sides of an industrial three-busbar bifacial PERC+ module, launched as the SolarWorld Sunmodule Protect 360° duo at Intersolar 2015 [33].

were carried out for various module-mounting surfaces having different albedo values. Fraunhofer ISE kindly provided these simulations, which used an in-house simulation package to calculate the annual energy yield of module installations, taking into account the local conditions of direct and diffuse light, ground reflection and shadowing effects.

Fig. 7 shows the simulated increase in annual energy yield for a PERC+ module with an STC front power of 270W and a bifaciality of 70%. In this simulation the modules were south oriented at a 30° tilt and landscape mounted, with several modules per row and a row pitch of 2.5m; a central location in Germany was also chosen. Depending on ground reflection, an increase of up to 25% in energy yield was predicted in the simulation. Note that normal grassland has an albedo of around 20%, whereas sand has an albedo of up to 40%. With optimized mounting systems, in combination with special reflective elements (e.g. white roof top foil), an albedo of up to 80% is possible.

Five bifacial PERC+ modules and one reference PERC module were installed in Freiberg, with a mounting configuration indicated by the yellow star in Fig. 7, and a predicted increase in energy yield of 5%. On the basis of the first measurements of these modules in June 2015, the PERC+ modules achieved a 5.5% higher energy yield than monofacial PERC reference modules. These outdoor measurements therefore provide an initial verification of the simulation, as well as reinforcing the increases in annual energy yield of bifacial PERC+ modules.

Conclusions and outlook

A novel industrial PERC solar cell design, given the name 'PERC+', which entails the screen printing of an Al rear metal grid instead of the conventional full-area aluminium rear metallization, has been introduced. The resulting Al finger grid, in combination with the five-busbar layout, corresponds to a metallization area fraction of 14.2%. Accordingly, the Al paste consumption of the PERC+ cells is considerably reduced to 0.15g per wafer, which compares with 1.6g per wafer for conventional PERC cells with a full-area Al layer. In contrast to conventional PERC cells, the PERC+ cells, because of the symmetric device structure, exhibit no wafer bow.

The specific Al grid line resistance has been determined to be 20±5μΩcm, which corresponds to a series resistance contribution of 0.1Ωcm^2 from the five-busbar Al finger grid.

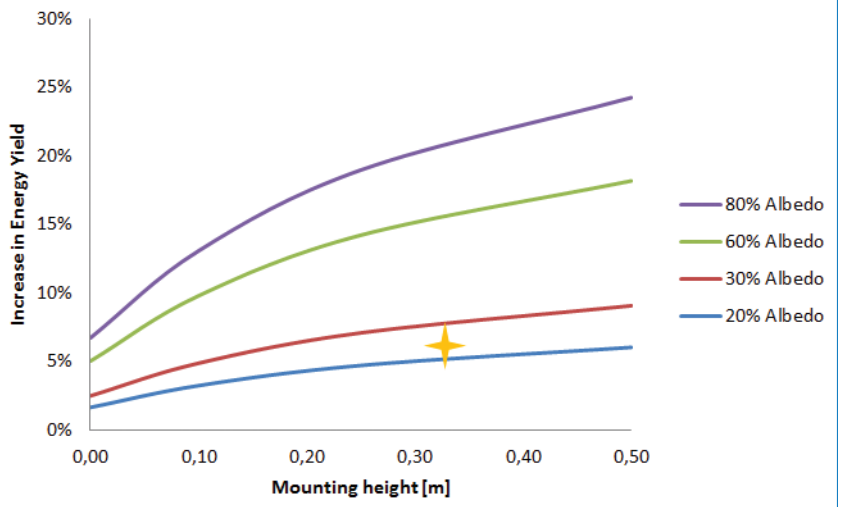

Figure 7. Simulated increase in annual energy yield for PERC+ modules compared with PERC modules, for various installation heights and albedo values of the ground at a central location in Germany. The yellow star indicates the installation conditions of the field test (grassland, 30cm above ground), with a predicted increase in energy yield of around 5%.

The slightly increased series resistance of the PERC+ cells decreases the efficiency by approximately 0.2% abs. Compared with full-area Al rear layers, the Al fingers confine the Si diffusion during furnace firing to the Al finger width; this leads to higher Si concentrations in the Al–Si melt, and hence to a deeper Al-BSF of 5.5µm, as opposed to 3.5µm for the full-area Al layer. The deeper Al-BSF reduces the rear contact recombination and hence increases the V_{oc} of PERC+ cells to 666mV, compared with 660mV for conventional PERC cells.

The PERC+ cells achieve front-side efficiencies, measured with a black chuck, of up to 21.2% and rear-side efficiencies of up to 16.6%, which equates to a bifaciality factor of 78%. PERC+ cells can therefore be used in bifacial module designs, such as the glass–glass module depicted in Fig. 8(a). The rear-side efficiency of 16.6% is limited mainly by the high Al metallization fraction of 14.2% and by the high reflection of the polished and passivated rear surface.

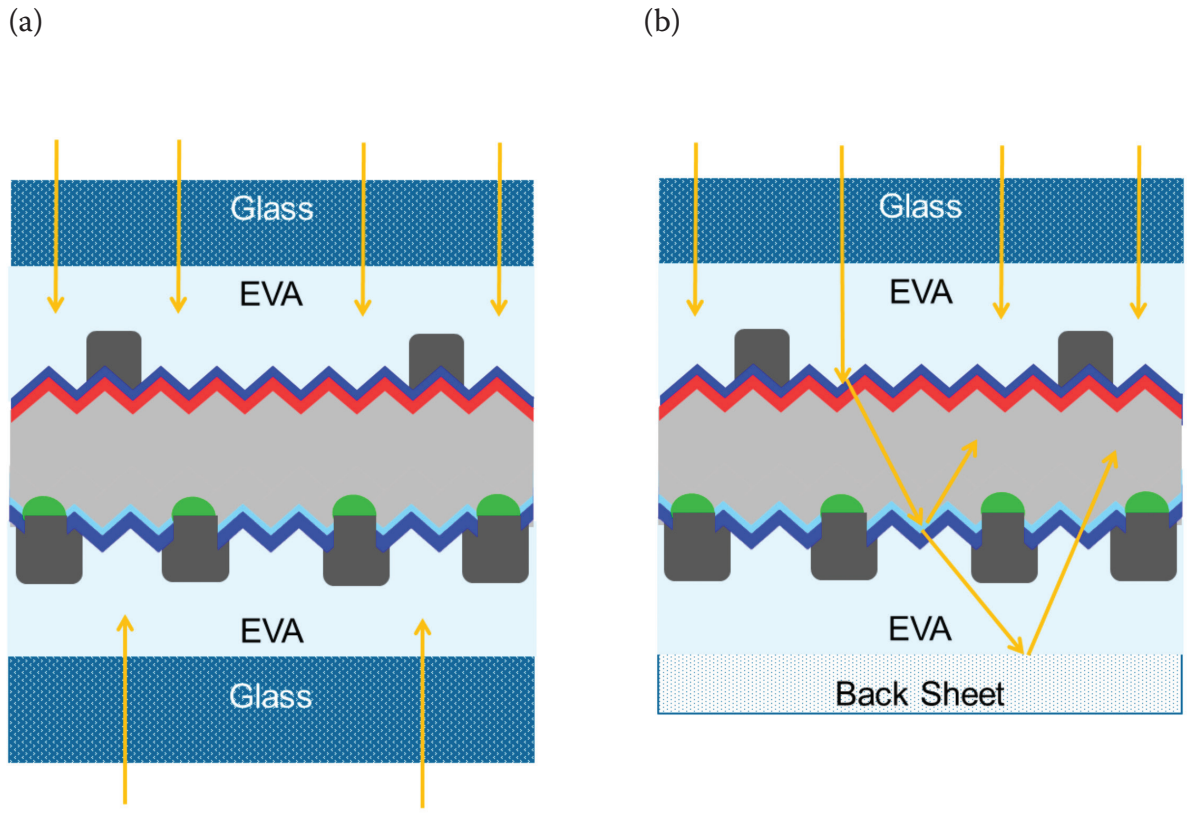

Figure 8. Schematic drawings of two potential applications of PERC+ solar cells: (a) bifacial glass–glass modules; (b) monofacial modules with a white backsheet, which serves as an external rear reflector for the PERC+ cells, leading to a higher effective rear reflectance compared with monofacial PERC cells (see Table 3).

"Bifacial modules incorporating PERC+ cells demonstrate an increase in annual energy yield between 5 and 25% in simulations."

When a white backsheet is placed at the rear of the PERC+ cell, similarly to the set-up of a conventional monofacial module, the white backsheet acts as an external rear reflector, increasing the rear reflectance of the PERC+ cells by 2.3%, to a value of 90.4%. Accordingly, when PERC+ cells are incorporated in a monofacial module with a white backsheet, as shown in Fig. 8(b), the higher Al grid resistance is compensated by the deeper Al-BSF and higher rear reflectance, leading to PERC+ efficiencies that are at least comparable to those of monofacial PERC cells. The best PERC+ efficiency is 21.5%, measured with a reflective brass chuck contacting the full Al finger grid. In summary, the PERC+ concept reduces the Al paste consumption by a factor of 10, enables bifacial applications, and performs on a par with conventional monofacial PERC cells when incorporated in monofacial modules with a white backsheet.

In addition to the results obtained at ISFH, a very similar bifacial PERC+ solar cell process has been independently developed by SolarWorld. To the authors' knowledge, SolarWorld is the first industry player to pioneer this cell technology employing an industrially relevant cell process. Novel glass–glass bifacial modules based on this cell technology and with a three-busbar layout were launched successfully at Intersolar 2015. These new bifacial modules incorporating PERC+ cells demonstrate an increase in annual energy yield of between 5 and 25% in simulations. The first outdoor measurements have been performed and corroborate the simulation results. Further development of the process is under way, with the aim of increasing front-side efficiencies and bifaciality.

Acknowledgements

We thank our ISFH colleagues K. Bothe, T. Brendemühl and T. Gandy for their help in obtaining the *I–V* measurements, and R. Brendel for his continued support of the industrial cell research at ISFH. Furthermore, we would like to acknowledge the support of D. Schulze and K. Meyer of SolarWorld in transferring the process to a mass-production environment and running the first pilot runs. Many thanks also to C. Reise from Fraunhofer-ISE for providing simulations of the annual energy yield of bifacial PERC+ modules under different installation conditions. Parts of this work were funded by the German Federal Ministry for Economic Affairs and Energy under Contract No. 0325716A.

References

[1] Fischer, G. et al. 2015, "Model based continuous improvement of industrial p-type PERC technology beyond 21% efficiency", *Proc. 5th SiliconPV*, Konstanz, Germany.

[2] SolarWorld 2015, Press Release (Mar.) [http://www.solarworld.de/en/group/investor-relations/news-announcements/corporate-news/single-ansicht/article/solarworld-expands-production-in-arnstadt/].

[3] Hanwha Q CELLS 2015, Press Release (Apr.) [http://investors.hanwha-qcells.com/releasedetail.cfm?ReleaseID=907243].

[4] Verlinden, P.J. et al. 2014, "Strategy, development and mass production of high-efficiency crystalline silicon PV modules", *Proc. 6th WCPEC*, Kyoto, Japan.

[5] Trina Solar 2015, Press Release (Jan.) [http://www.pv-tech.org/news/trina_solar_starts_perc_technology_volume_production].

[6] SEMI PV Group Europe 2015, "International technology roadmap for photovoltaic (ITRPV): 2014 results", 6th edn (Apr.) [http://www.itrpv.net/Reports/Downloads/].

[7] Blakers, A.W. et al. 1989, "22.8% efficient silicon solar cell", *Appl. Phys. Lett.*, Vol. 55, pp. 1363–1365.

[8] Guo, S. et al. 2013, "Vertically mounted bifacial photovoltaic modules: A global analysis", *Energy*, Vol. 61, pp. 447–454.

[9] Janssen, G.J.M. et al. 2015, "Outdoor performance of bifacial modules by measurements and modelling", *Proc. 5th SiliconPV*, Konstanz, Germany.

[10] Romijn, I.G. et al. 2013, "Industrial cost effective n-PASHA solar cells with >20% cell efficiency", *Proc. 28th EU PVSEC*, Paris, France, pp. 736–740.

[11] Song, D. et al. 2012, "Progress in n-type Si solar cell and module technology for high efficiency and low cost", *Proc. 38th IEEE PVSC*, Austin, Texas, USA, pp. 3004–3008.

[12] Mihailetchi, V.D. et al. 2010, "Screen printed n-type silicon solar cells for industrial application", *Proc. 26th EU PVSEC*, Hamburg, Germany, pp. 1446–1448.

[13] Larionova, Y. et al. 2015, "Industrial ion implanted co-annealed and fully screen-printed bifacial n-PERT solar cells with low-doped back-surface fields", Presentation at 5th nPV Worksh., Konstanz, Germany.

[14] Taguchi, M. et al. 2014, "24.7% record efficiency HIT solar cell on thin silicon wafer", *IEEE J. Photovolt.*, Vol. 4, pp. 96–99.

[15] Strahm, B. et al. 2014, "The Swiss Inno-HJT project: Fully integrated R&D to boost Si-HJT module performance", *Proc. 29th EU PVSEC*, Amsterdam, The Netherlands, pp. 467–471.

[16] Steckemetz, S. et al. 2001, "Thin Cz-silicon solar cells with rear silicon nitride passivation and screen printed contacts", *Proc. 17th EU PVSEC*, Munich, Germany, pp. 1902–1905.

[17] Cesar, I. et al. 2008, "Benchmark of open rear side solar cell with improved Al-BSF process at ECN", *Proc. 23rd EU PVSEC*, Valencia, Spain, pp. 1770–1775.

[18] Vermont, P. et al. 2012, "Spatial ALD Al2O3 film integrated in low-cost, high-performance bifacial solar cells", *Proc. 27th EU PVSEC*, Frankfurt, Germany, pp. 1757–1760.

[19] Teppe, A. et al. 2014, "Novel technology approach based on standard quality mc wafer achieving solar cell efficiencies significantly above 18% in an industrial production environment", *Proc. 29th EU PVSEC*, Amsterdam, The Netherlands, pp. 1310–1313.

[20] Teppe, A. et al. 2015, "Bifacial multicrystalline solar cells with efficiencies above 18% processed in an industrial production environment", *Proc. 30th EU PVSEC*, Hamburg, Germany.

[21] Hannebauer, H. et al. 2014, "21.2%-efficient fineline-printed PERC solar cell with 5 busbar front grid", *physica status solidi (RRL)*, Vol. 8, pp. 675–679.

[22] Dullweber, T. et al. 2014, "Fine-line printed 5 busbar PERC solar cells with conversion efficiencies beyond 21%", *Proc. 29th EU PVSEC*, Amsterdam, The Netherlands, pp. 621–626.

[23] Dullweber, T. et al. 2015, "PERC+: Industrial PERC solar cells with rear Al grid enabling

bifaciality and reduced Al paste consumption", *Prog. Photovoltaics Res. Appl.* [forthcoming].
[24] Urrejola, E. et al. 2011, "Silicon diffusion in aluminum for rear passivated solar cells", *Appl. Phys. Lett.*, Vol. 98, p. 153508.
[25] Müller, J. et al. 2012, "Modeling the formation of local highly aluminum-doped silicon regions by rapid thermal annealing of screen-printed aluminum", *physica status solidi (RRL)*, Vol. 6, pp. 111–113.
[26] Lauermann, T. et al. 2013, "Diffusion-based model of local Al back surface field formation for industrial passivated emitter and rear cell solar cells", *Prog. Photovoltaics Res. Appl.*, Vol. 23, pp. 10–18.
[27] Gatz, S. et al. 2012, "Analysis and optimization of the bulk and rear recombination of screen-printed PERC solar cells", *Energy Procedia*, Vol. 27, pp. 95–102.
[28] Dullweber, T. et al. 2013, "Silicon wafer material options for highly efficient p-type PERC solar cells", *Proc. 39th IEEE PVSC*, Tampa, Florida, USA, pp. 3074–3078.
[29] Dullweber, T. et al. 2015, "The PERC+ cell: A 21%-efficient bifacial PERC solar cell", *Proc. 30th EU PVSEC*, Hamburg, Germany.
[30] Saint-Cast, P. 2012, "Passivation of Si surfaces by PECVD aluminum oxide", Ph.D. dissertation, University of Konstanz, Germany.
[31] Brendel, R. et al. 1996, "Quantum efficiency analysis of thin-layer silicon solar cells with back surface fields and optical confinement", *IEEE Trans. Electron Dev.*, Vol. 43, pp. 1104–1113.
[32] *Handelsblatt* 2014, "Asbeck versucht Neustart", Newspaper Article (Dec. 15).
[33] SolarWorld 2015, Press Release (May) [http://www.pv-tech.org/news/intersolar_europe_solarworld_to_launch_glass_glass_bifacial_modules].

About the Authors

Dr. Thorsten Dullweber leads the industrial solar cells R&D group at ISFH. His research focuses on high-efficiency industrial-type PERC silicon solar cells and ultra-fine-line screen-printed Ag front contacts. Before joining ISFH in 2009, Dr. Dullweber worked for nine years as a project leader in the microelectronics industry at Siemens AG and later at Infineon Technologies AG.

Christopher Kranz received his diploma degree in physics from the University of Münster in 2011, after which he started a Ph.D. programme at ISFH in the industrial solar cells R&D group. He currently carries out research on screen-printed solar cells with passivated emitter and rear side.

Dr. Robby Peibst received his diploma degree in technical physics in 2005. In 2010 he received his Ph.D. from the Leibniz University of Hanover, with a thesis on germanium-nanocrystal-based memory devices. He joined ISFH in 2010 and has led the emerging solar technologies group since 2013. His research focuses on the development of techniques enabling the production of high-efficiency silicon solar cells.

Ulrike Baumann graduated in 2011 as a laboratory technical assistant in chemistry, after which she joined the industrial solar cells R&D group at ISFH, where she is in charge of processing industrial PERC solar cells. She is also responsible for the optimization and maintenance of a production-type wet-chemical batch processing tool.

Helge Hannebauer studied technical physics at the Leibniz University of Hanover from 2005 to 2009. The work for his diploma thesis, carried out at ISFH, involved the optimization of screen-printed solar cells. In 2010 he started his Ph.D. at ISFH, focusing on advanced screen printing and selective emitters.

Alexander Fülle received his diploma degree in technical physics from the University of Applied Sciences Zwickau (FH) in 2006, after which he spent two years in the microsystems department there. Since 2008 he has been working at SolarWorld, where he leads the process integration team.

Stefan Steckemetz received his diploma in technical physics from the University of Applied Sciences Aachen in 1993. He then worked on crystalline Si solar cells at ISFH and Sunways AG, and joined SolarWorld in 2006, where he focuses on screen-printing metallization for high-efficiency solar cells.

Torsten Weber received his diploma degree in physics from the University of Hanover in 2006. He currently works as a senior R&D engineer at SolarWorld, where his research and expertise focus on the transfer and integration of high-efficiency solar cell and module concepts, from the laboratory scale to high-volume production.

Dr. Matthias Müller received his diploma degree in physics from Leipzig University in 2009, followed by his Ph.D. from Leibniz University Hanover in 2014. From 2007 he worked for Q-Cells SE, GP Inspect GmbH and Magdeburg-Stendal University of Applied Sciences, before joining SolarWorld in 2011, where he is responsible for numerical device simulation.

Dr. Phedon Palinginis leads the solar cell development group at SolarWorld. Before joining the company in 2006, he investigated dipole and spin coherences in semiconductor nanostructures as a doctoral/postdoctoral researcher at the Universities of Oregon and California (Berkeley). He holds a degree in physics from the University of Karlsruhe.

Dr. Holger Neuhaus received his degree in physics and his Ph.D. from the Universities of Hanover and New South Wales in 1998 and 2002 respectively. He then worked at Pacific Solar as a characterization engineer. In 2003 he joined the SolarWorld Group, and since 2009 he has been the MD of its R&D organization.

Enquiries

Thorsten Dullweber
Institute for Solar Energy Research Hamelin (ISFH)
Am Ohrberg 1
D-31860 Emmerthal
Germany

Tel: +49-5151-999-638
Email: t.dullweber@isfh.de
Website: www.isfh.de